

TECHNICAL VETTING OF FREE-FALL CONE PENETROMETER

P Jeanjean

BP America, Inc, Houston, USA

D Spikula and A Young

Geoscience, Earth and Marine Services, Inc, Houston, USA

Abstract

The paper describes the vetting process to validate a new free-fall cone penetration test (CPT) tool. First, the analytical model to calculate the dynamic embedment of the tool is described, and the model predictions are compared with laboratory and field tests results. Then the tip resistance and pore pressure measured with the new tool are compared to those measured with conventional methods at two Gulf of Mexico deepwater sites. The paper demonstrates that the dynamic embedment depth of the new CPT tool can be reliably predicted and that the tool measurements compare well with those of conventional seabed-based methods.

1. Introduction

1.1 Purpose of the new tool

An innovative cone penetration test (CPT) rig was recently developed, and is extensively described in Young et al. (2011). The tool is deployed from non-drilling vessels and dynamically inserted into the seabed using conventional jumbo piston coring (JPC) deployment techniques. A CPT rod, which is located inside the JPC core barrel during deployment, is then monotonically pushed into the seabed below the CPT barrel. Two types of barrel, 11.6m (short-barrel) and 17.7m (long-barrel), are available. In 2011, the suite of tools was further expanded to include a seabed unit. For this unit, the CPT is not penetrated dynamically into the seabed but starts a monotonic push at the seafloor (Figure 1).

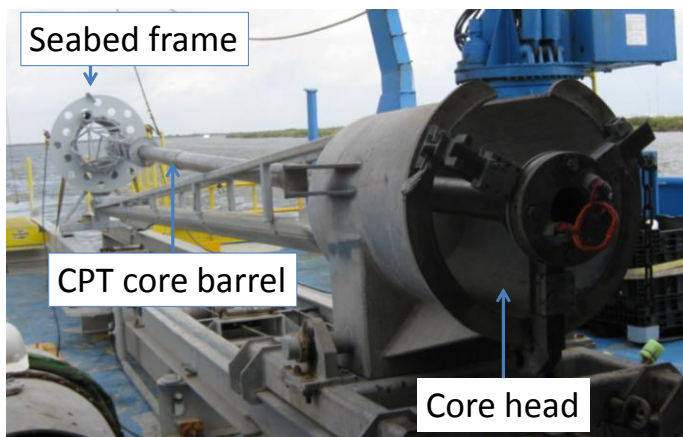


Figure 1: CPT seabed unit on deck of deployment vessel (courtesy of B Bernard, TDI-Brooks)

Because the CPT rod is entirely housed inside the barrel, the depth interval to which CPT data can be acquired cannot be greater than the length of the barrel. However, by carefully planning the dynamic penetration of the tool, overlapping CPT profiles can be obtained down to a depth of about 40m, thereby generating a composite continuous CPT profile from the seafloor to the depth of interest. The CPT data can then be calibrated in the top 15–18m with shear strength measurements from JPC samples.

This strategy in combining the available data is illustrated in Figure 2. Not all the data in Figure 2 need to be acquired at all locations of interest, as judicious acquisition of a dataset is encouraged.

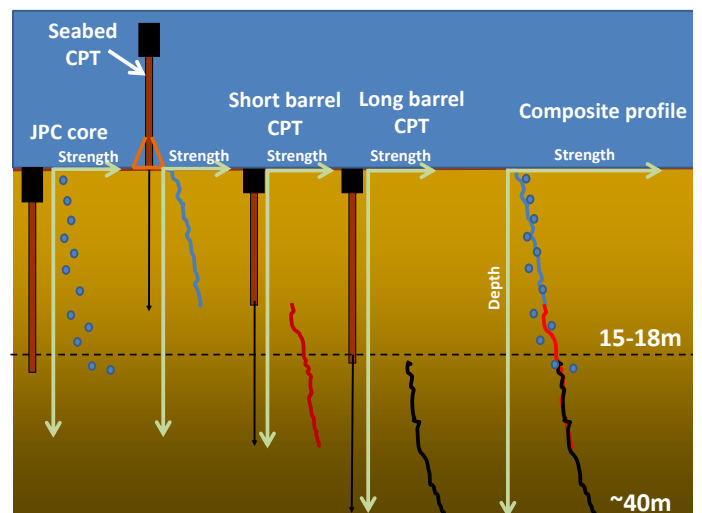


Figure 2: Combining JPC, seabed CPT, short-barrel CPT and long-barrel CPT data to obtain a composite strength profile

The ability to correctly predict the embedment of the CPT tool is critical in ensuring that there is a depth interval where the short-barrel CPT data can be overlaid with the JPC data and long-barrel CPT data. The following section details the development of the embedment prediction model.

2. Development of Penetration Model

2.1 Formulation of the model

The key publications used to develop the penetration model herein include True (1976) and O'Loughlin et al. (2004). The forces acting on a typical anchor penetrator and the free-fall CPT penetrator are shown in Figure 3.

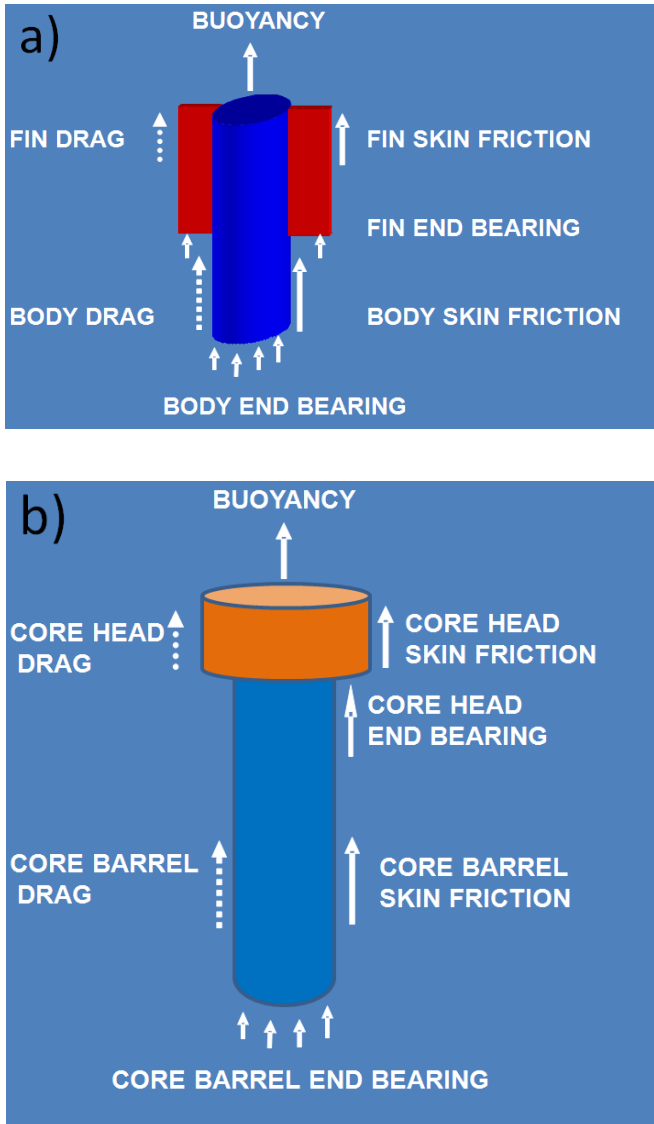


Figure 3: Forces acting on (a) a typical anchor penetrator; and (b) the free-fall CPT rig penetrator

These forces are expressed in two sets of equations. In water, the governing equation of motion is taken as:

$$m \frac{d^2z}{dt^2} = mg - F_{bw} - F_{dw} \quad (1)$$

where m is the mass of penetrator; z is depth; t is time; g is acceleration of gravity; F_{bw} is the buoyancy force in water with $F_{bw} = \rho_w g V$, ρ_w is the density of water; V is the volume of penetrator; F_{dw} is the inertial drag force of water with $F_{dw} = \frac{1}{2} C_{df} \rho_w A_p \frac{dz}{dt}^2$; C_{df} is the fluid drag coefficient; and A_p is the frontal projected area of penetrator.

In soil, the governing equation of motion is taken as:

$$m \frac{d^2z}{dx^2} = mg - F_{bs} - F_p - F_s - F_{ds} \quad (2)$$

where, in addition to previously defined variables, F_{bs} is the buoyancy force in the soil with $F_{bs} = \rho_s g V$, ρ_s is density of soil; F_p is the soil end bearing resistance of all surfaces perpendicular to the penetrator trajectory with $F_p = R_f \sum_i N_{c,i} S_{u,i} A_{p,i}$; R_f is the strain rate factor with $R_f = 1 + \lambda \log \frac{dz}{V_s}$; λ is strain rate multiplier; V_s is the reference velocity; $N_{c,i}$ is the bearing capacity factor for i^{th} surface; $S_{u,i}$ is the shear strength at depth of i^{th} surface; $A_{p,i}$ is the area of i^{th} surface; F_s is the soil skin friction resistance of all surfaces parallel to the penetrator trajectory with $F_s = R_f \sum_n \alpha_n S_{u,n} A_{s,n}$; α_n is the adhesion factor for n^{th} surface; $A_{s,n}$ is the area of n^{th} surface; F_{ds} is the inertial drag force with $F_{ds} = \frac{1}{2} C_d \rho_s A_p \frac{dz}{dt}^2$; C_d is the drag coefficient with $C_d = C_{ds} + \frac{C_{df} - C_{ds}}{1 + \vartheta^f}$; C_{df} is fluid drag coefficient; C_{ds} is the soil drag coefficient; and $\vartheta^f = \frac{F_{ds}}{F_p + F_s}$. This model was implemented in a Microsoft[®] Excel spreadsheet and is solved via finite difference techniques with a time interval of 10ms.

2.2 Small-scale laboratory experiments

In 2006, a series of small-scale experiments were performed in the C&C Technologies laboratory in Houston, USA. Three types of penetrators, as shown in Figure 4, were dropped and allowed to free fall into a tub of reconstituted Gulf of Mexico clay. The models were 0.5m long with a shaft diameter of 31mm and a mass of 2kg. They had fins for over 80%, 60%, and 40% of their length, and had an interchangeable nose section which could be round, angled at 30°, or angled at 60° (Figure 4). Nine penetrators were therefore available.

The soil bed was made of reconstituted Gulf of Mexico clay, which was thoroughly mixed and let to reconsolidate for two weeks. The clay had a plasticity index of 56, an average water content of 85%, a shear strength of about 1.8kPa (as measured with T-bar and minivane tests) and a sensitivity of 1.5. A T-bar test was run immediately before each test.



Figure 4: Model penetrators tested in Gulf of Mexico clays

The shaft section of the penetrators was hollow and contained an on-board instrumentation package, which included one accelerometer and one inclinometer, as shown in Figure 5.



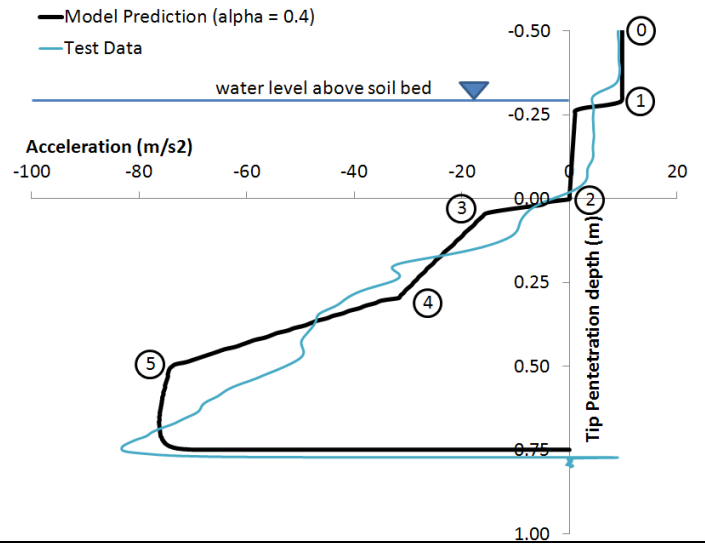
Figure 5: Model penetrators instrumentation package

The analytical model (Equations 1 and 2) was used with the input parameters of Table 1. The side adhesion factor (α) was varied until the predicted embedment depth matched the measured embedment depth. The reference velocity (V_s) is representative of typical direct simple shear (DSS) testing conditions.

Table 1: Input parameters for anchor penetration model

Parameters	Value
Side adhesion factor, α	0.4
Body end bearing factor, N_{cb}	9
Fin end bearing factor, N_{cf}	7.5
Fluid drag coefficient, C_{df}	0.57
Soil drag coefficient, C_{ds}	0.7
Strain rate multiplier, λ	0.1
Reference velocity, V_s (m/s)	1.0E-7

A typical measured acceleration profile during the anchor dynamic penetration is shown in Figure 6. The predicted profile is also shown and captures key phases of the penetration.



- ① anchor is falling in air
- ① anchor nose hits air/water interface
- ② anchor nose hits water/soil interface
- ③ anchor nose is entirely penetrated
- ④ fins start to embed into soil
- ⑤ top of anchor is at soil/water interface (i.e. anchor is embedded over its entire length)

Figure 6: Example of measured and predicted acceleration record during penetration

The measured penetration depths for all tests compare favourably with the predicted ones (Figure 7). The ratio of measured over-predicted penetration depths has a mean of 0.98 and a coefficient of variation (COV) of 0.05.

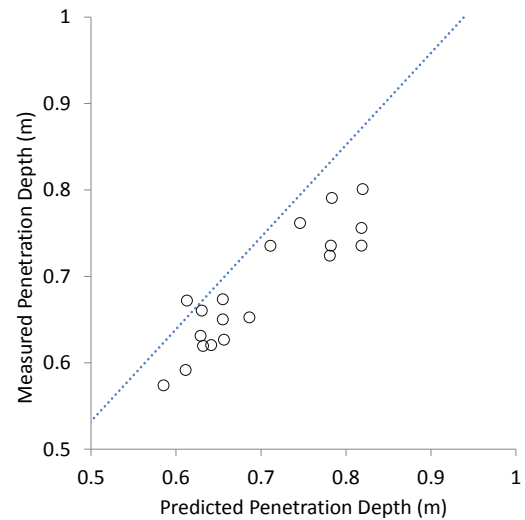


Figure 7: Measured versus predicted final penetration depth for small-scale laboratory penetration tests

2.3 Verification with large-scale field data

The analytical model was then tested against two sets of full-scale tests results: the Deep Ocean Model Penetrator (DOMP) experiments and torpedo anchor tests by Petrobras. The DOMP experiments (Freeman and Burdett, 1986) were conducted to study the feasibility of burying radioactive waste in deep

ocean sediments through free-falling penetrators. The soil strength profile for DOMP I tests is $(1.7 + 1.0z)$ kPa, and the soil strength profile for DOMP II tests is $(5.4 + 1.1z)$ kPa, where z is the depth in metres. Figure 8 illustrates the designs and scale of the penetrators used in the DOMP II field tests.

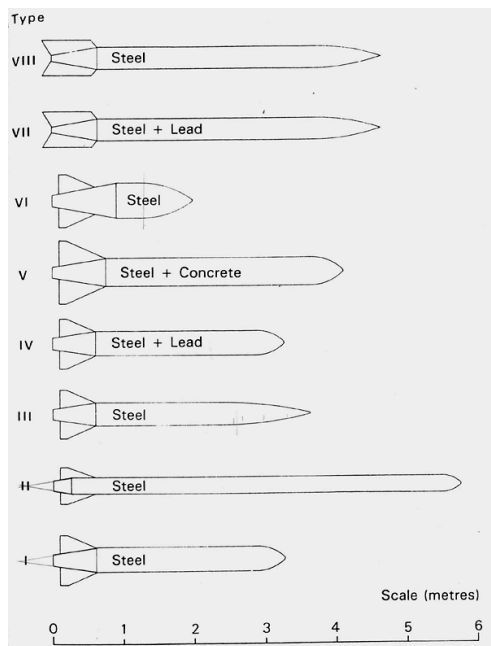


Figure 8: Shape and size of penetrators used in the DOMP II field tests (Freeman and Burdett, 1986)

Medeiros (2002) reports the results of field tests with torpedo anchors developed by Petrobras. For a torpedo anchor weighing 400kN (dry), 12m long and with a 0.76m outside diameter (OD), the medium penetration was 29m at a drop height of 30m in normally consolidated clay with shear strength equal to $(5 + 2z)$ kPa. Additional publications of installation records for other types of penetrators, such as the OMNI-Max anchor (Zimmerman et al., 2009), or deep penetrating anchors (Sturm et al., 2011; O’Loughlin et al., 2004) do not offer a complete set of information in order to verify the model herein.

The penetration model was used with the same values shown in Table 1 to hindcast the final penetration depths of the DOMP and torpedo penetrators. The only exception was the numerical values of the fluid drag coefficient (C_{df}), which depends on the shape of the penetrator. A value of $C_{df} = 0.33$, as quoted by Fernandes et al. (2005), was used to hindcast the results of Medeiros (2002). Values of C_{df} between 0.1 and 0.2 were used for the DOMP I and II tests, depending on the penetrator.

As illustrated in Figure 9, the prediction model performed well, with the same side adhesion factor (α) of 0.4. The measured penetration depths were about 15% higher than the predictions.

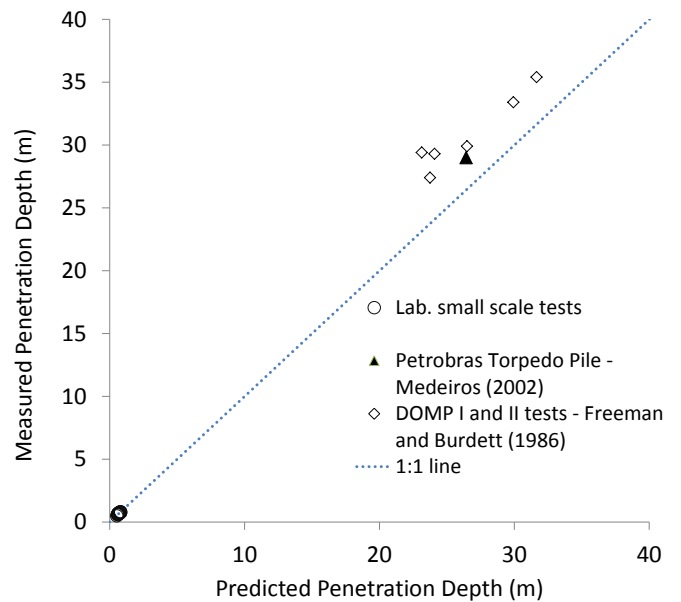


Figure 9: Measured versus predicted final penetration depth for DOMP tests and torpedo anchor test

3. Prediction of Free-Fall CPT Penetration Depth

3.1 Free-fall CPT geometry and test setup

The geometry of the free-fall CPT penetrator is shown in Figure 10 during the dynamic penetration into the soil.

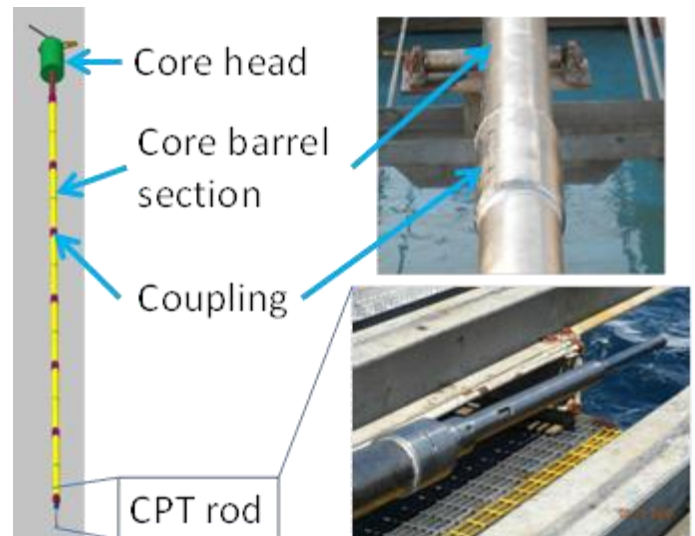


Figure 10: Geometry of free-fall CPT during dynamic penetration

The CPT rig is typically released (or triggered) only 1m or so above the seafloor, with little free fall in the water column. The CPT data acquisition module records time, acceleration, tip resistance, pore pressure and sleeve resistance during free fall and the subsequent monotonic push.

3.2 Predicted and measured deceleration

Figure 11 shows an example of measured acceleration profile during a typical deployment and the corresponding model predictions.

Table 2: Input parameters for free-fall CPT penetration model

Parameters	Value
Side adhesion factor, α	varies
Core barrel end bearing factor, N_{cb}	9
Core head end bearing factor, N_{ch}	9
Fluid drag coefficient, C_{df}	1.0
Soil drag coefficient, C_{ds}	0.7
Strain rate multiplier, λ	0.1
Reference velocity, V_s (m/s)	1.0E-7

To simplify the prediction process, an α factor of 0.4 is proposed for the short-barrel deployments and an α of 0.2 is proposed for the long-barrel deployments. Figure 12 shows that good agreement is obtained if these values are used. The ratio of measured over-predicted embedment depth is 0.98 on average for the 24 CPT deployments.

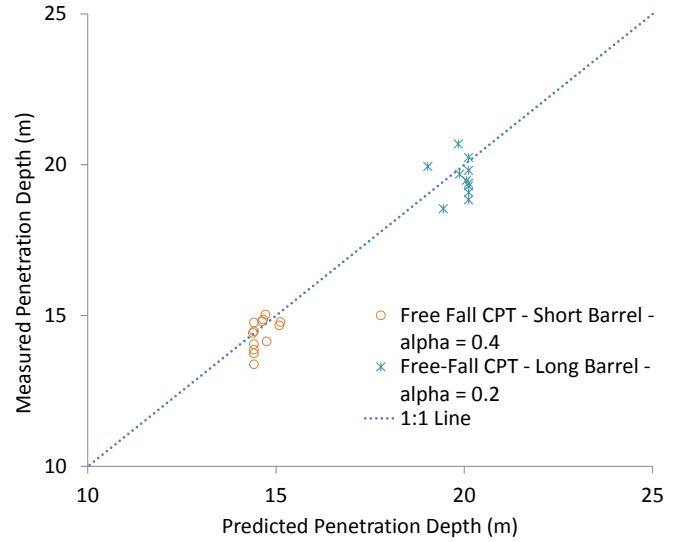


Figure 12: Measured versus predicted free-fall CPT penetration depths for 24 deployments

3.5 Overall performance of penetration model

The global performance of the prediction model is shown in Figure 13. All the tests have been hindcast with an α value of 0.4, except for the long-barrel CPT drops, which have been hindcast with an α value of 0.2. The lower side adhesion factor (α) value for the long-barrel drops is believed to be the result of continuous water entrapment at the barrel/soil interface as the CPT barrel continues to penetrate to deeper depths.

Indirect evidence of water entrapment at the soil/penetrator interface was observed during the laboratory small-scale tests. The penetrators were first dropped completely in air, without a water layer above the soil bed. The best-fit side adhesion factor (α) to hindcast the penetration depths of these tests was 0.7, which corresponds roughly to the inverse of

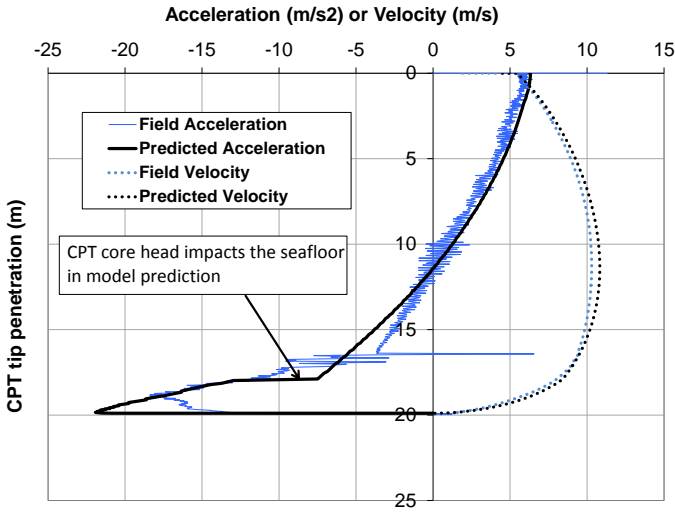


Figure 11: Typical example of measured and predicted acceleration profile for a CPT deployment; the model is tweaked until the correct final penetration is calculated (with $\alpha = 0.2$ in this example)

As can be seen, the initial acceleration after the CPT is released is not equal to the acceleration of gravity (g). Experience indicates that the initial acceleration is about 75% of g , and the initial velocity is in the order of 1–2m/s (Bernard, 2012). In addition, it can be observed that the model will predict a sharp break in acceleration when the core head impacts the seafloor.

However, the measured data suggest that the acceleration profile is perturbed even when the core head is still a few metres above the seafloor. In Figure 11, the acceleration starts decreasing at a CPT tip penetration of 16m, although the core head physically penetrates the seafloor only when the tip is at a penetration depth of 17.7m. This occurs because the pendant wire is getting taut prior to the core head reaching the seafloor (Bernard, 2012).

3.4 Predicted and measured penetration depths

The penetration depth of the free-fall CPT rig was hindcast for 13 short-barrel deployments and 11 long-barrel deployments using the parameters in Table 2. These parameters are similar to the parameters in Table 1, except for the fluid drag coefficient. This coefficient has little effect on the calculated penetration depth because the velocities of the CPT rig in water are low.

Only the side adhesion factor (α) was varied in order to empirically match the observed penetration of the CPT rig. For the long-barrel deployments, hindcast α values ranged from 0.16 to 0.27 with a mean of 0.22 and a COV of 16%. For the short-barrel deployments, hindcast α values ranged from 0.36 to 0.54, with a mean of 0.42 and a COV of 13%.

the soil sensitivity ($1/1.5 = 0.67$). However, when a 0.3m layer of water was added on top of the soil bed, the best-fit α (as previously described) dropped to 0.4. This suggests that water was being entrapped along the penetrator surface during penetration, even though that surface was relatively smooth and free of major protuberances. This increase in water in the soil reduces the steel/soil friction to a value below that of the soil remolded shear strength.

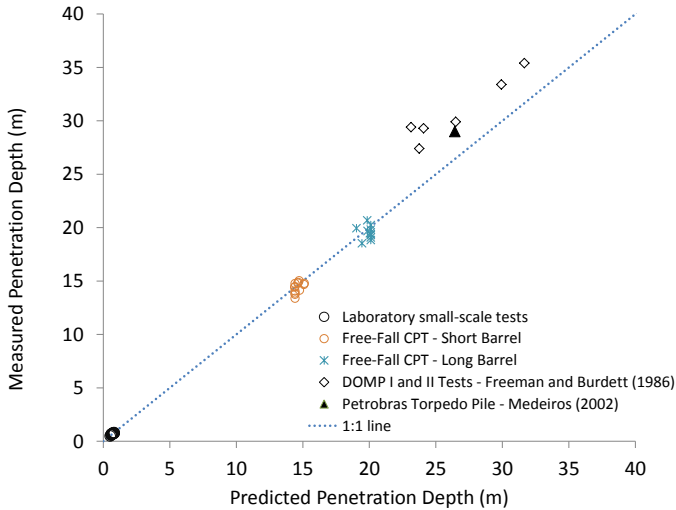


Figure 13: Measured versus predicted penetration depths for all penetrators analysed

It should be noted that the CPT barrel is not smooth but is made of 3m (10ft) sections with an external diameter of 0.14m. These sections are connected to each other with couplings that have an external diameter of 0.16m (see Figure 10). These protruding couplings are speculated to exacerbate water entrapment at the soil/barrel interface, thereby resulting in a decreased friction at a given depth as an increasing length of barrel penetrates past that depth.

The overall performance of the prediction model is robust for the database herein, and allows confident calculation of the CPT rig dynamic final penetration depth.

4. Comparison of Free-Fall CPT Data with Conventional Systems

4.1 Description of validation sites

The proper performance of the free-fall CPT tool sensors was verified and validated by comparing the cone tip resistance, pore pressure and sleeve friction resistance obtained with this tool with those acquired by conventional seabed CPT systems.

Two validation sites were selected in deepwater Gulf of Mexico. In the top 18m, the first site consists of

uninterrupted parallel-bedded hemiplegic sediments that have not been affected by erosion, faulting or mass wasting events. These sediments are underlain by debris flow deposits down to the termination depths of the CPTs (Figure 14).

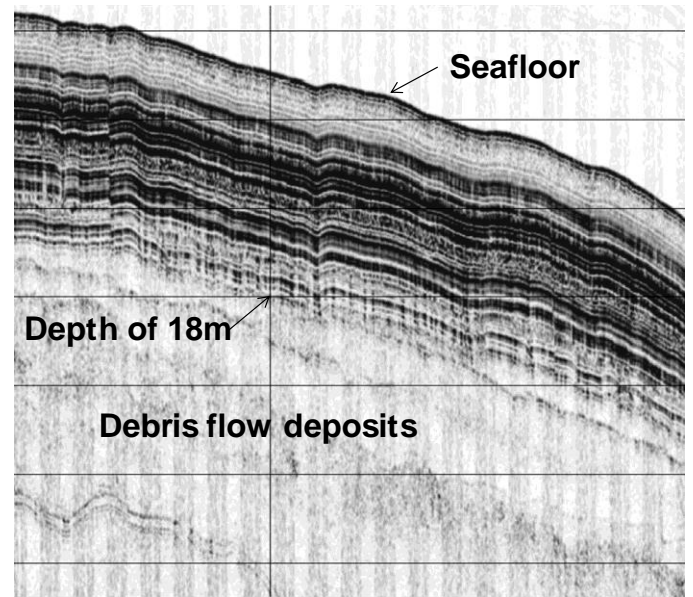


Figure 14: Sub-bottom profiler record at calibration site 1

The second calibration site consisted of parallel-bedded hemiplegic sediments interbedded with thin mass wasting events down to 22m (Figure 15). At that depth, an erosional unconformity was present, with an unknown thickness of sediments having been removed. At both sites, the free-fall CPT data was acquired at a seafloor location within 20m of where the conventional seabed-CPT test was performed.

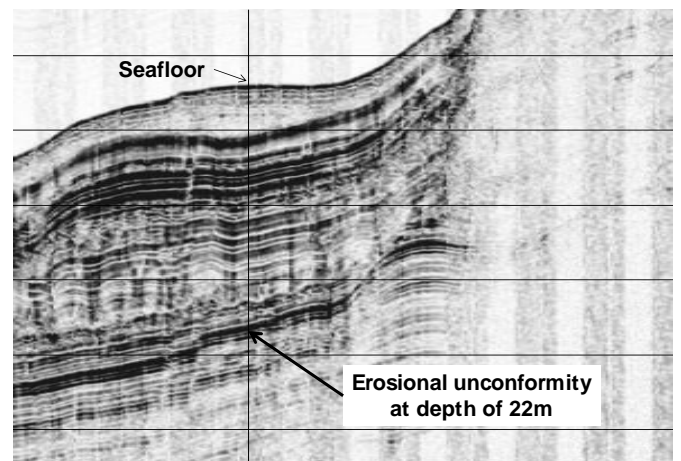


Figure 15: Sub-bottom profiler record at calibration site 2

4.2 Comparison of tip resistance and pore pressure TDI-Brooks, Inc, performed the free-fall CPT tests and provided the results as a 'Class A' prediction (i.e. without knowledge of the data acquired by conventional seabed CPT tools). Figure 16 shows the comparison of the corrected cone tip resistance and

pore pressure response between the free-fall CPT and the conventional seabed CPT rig at site 1.

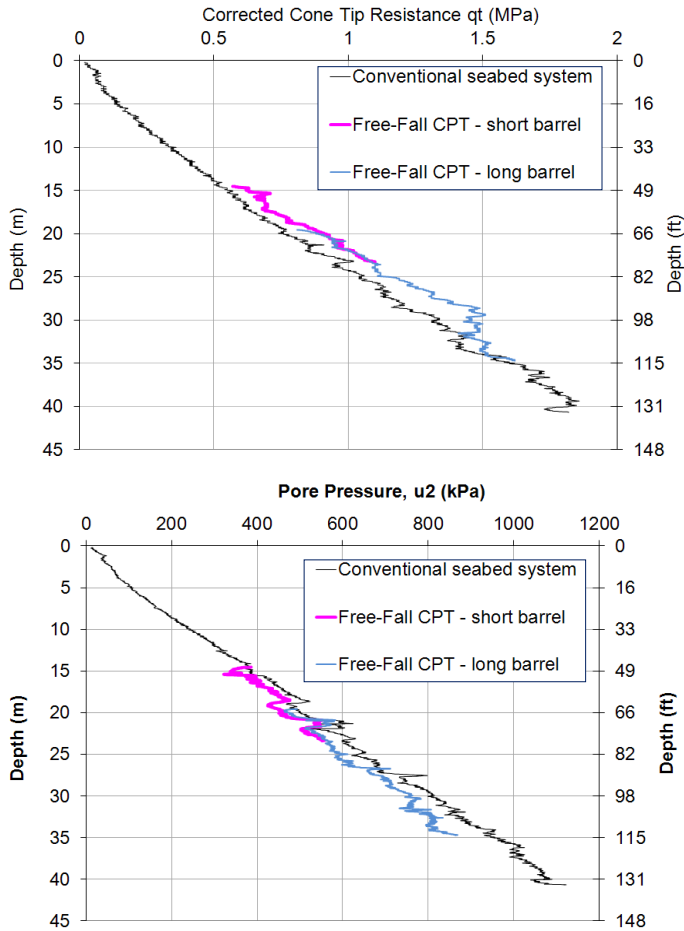


Figure 16: Comparison of CPT tip resistance and pore pressure between free-fall CPT and conventional systems at site 1

Figure 17 shows the comparison of corrected cone tip resistance and pore pressure response between the free-fall CPT and the conventional seabed CPT system at site 2. During the monotonic push, the measured tip resistance and pore pressure compared very well between the two systems. At site 1, the free-fall CPT corrected tip resistance was, on average, 12% higher than that of the conventional system. A comparison between the free-fall CPT sleeve friction measurements and those of the conventional system is not presented because the free-fall CPT friction sleeve did not provide reliable measurements at these two sites.

5. Conclusions

This paper describes the technical validation process of the new free-fall CPT (the ‘CPT Stinger’; Young et al., 2011). First, a rigorous analytical model initially developed for deepwater gravity anchors was modified and calibrated to predict the dynamic final penetration of the CPT. A single parameter, the side adhesion factor (α) was varied to match the measured penetration depths of 24 deployments, and α values

of 0.2 and 0.4, respectively, are recommend to predict the behaviour of the long- and short-barrel CPTs.

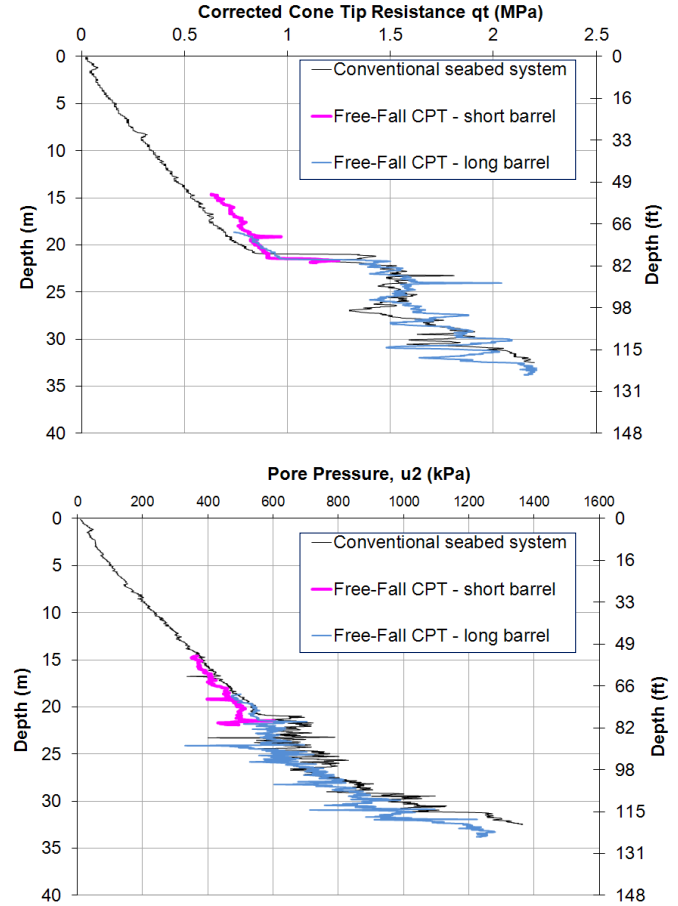


Figure 17: Comparison of CPT tip resistance and pore pressure between free-fall CPT and conventional systems at site 2

Second, the tip resistance and pore pressure measurements obtained with this tool compared very well with measurements obtained with conventional seabed-based systems at two Gulf of Mexico deep-water sites. The authors therefore believe that this new CPT tool can reliably acquire CPT data at predominantly soft clay sites, which can be judiciously incorporated into new strategies to acquire fit-for-purpose geotechnical data in the top 40m below the seafloor.

Acknowledgments

The small-scale laboratory penetrator tests described herein were conducted in 2005 and 2006 in the C&C Technologies laboratory in Houston, Texas, under the direction of Steve Garmon. His ingenuity and willingness to experiment are gratefully acknowledged. Dr Bernie Bernard, TDI-Brooks, Inc, is acknowledged for the passion and enthusiasm he displayed throughout the development and validation of the free-fall CPT rig. The authors are grateful to BP America, Inc, for permission to publish.

References

- Bernard B. (2012). Personal communication.
- Fernandes AC, de Araujo JB and Diniz RG. (2005). Hydrodynamic aspects of the Torpedo anchor installation. Proceedings OMAE 2005, Halkidiki, Greece, Paper OMAE 2005-67201.
- Freeman TJ and Burdett JRF. (1986). Deep ocean model penetrator experiments. Commission of the European Communities Nuclear Science and Technology series, Report No. EUR10502.
- Medeiros CJ. (2002). Low cost anchor system for flexible risers in deep water. OTC 14151. Proc. Offshore Tech. Conf., Houston, USA.
- O'Loughlin CD, Randolph MF and Richardson M. (2004). Experimental and theoretical studies of deep penetrating anchors. OTC 16841. Proc. Offshore Tech. Conf., Houston, USA.
- Sturm H, Lieng JT and Saygili G. (2011). Effect of soil variability on the penetration depth of dynamically installed drop anchors. OTC 22396. Proc. Offshore Tech. Conf., Houston, USA.
- True DG. (1976). Undrained vertical penetration into ocean bottom soils. PhD Thesis, University of California, Berkeley.
- Young A, Bernard B, Remmes B, Babb L and Brooks J. (2011). "CPT Stinger" – An innovative method to obtain CPT data for integrated geoscience studies. OTC 21569. Proc. Offshore Tech. Conf., Houston, USA.
- Zimmerman E, Smith M and Shelton JT. (2009). Efficient gravity installed anchor for deepwater mooring. OTC 20117. Proc. Offshore Tech. Conf., Houston, USA.